ACS Photonics

Letter

pubs.acs.org/journal/apchd5

Room-Temperature, Solution-Processed MoO_x Thin Film as a Hole Extraction Layer to Substitute PEDOT/PSS in Polymer Solar Cells

Bohao Li,[†] He Ren,[†] Hongyi Yuan, Alamgir Karim, and Xiong Gong*

College of Polymer Science and Polymer Engineering, The University of Akron, Akron, Ohio 44325, United States

ABSTRACT: Room-temperature, solution-processed molybdenum oxide (MoO_x) as a hole extraction layer to substitute PEDOT/PSS in polymer solar cells was demonstrated. The thin film of MoO_x shows a smoother surface, better transparency, and high electrical conductivity than that of PEDOT/PSS thin layer and, thus, leading enhanced efficiency of PSCs than those using PEDOT/PSS anode buffer layer. These results demonstrated that the utilization of room-temperature, solution-processed MoO_x thin film as a hole extraction layer in polymer solar cells blaze a trail to achieve high performance devices.

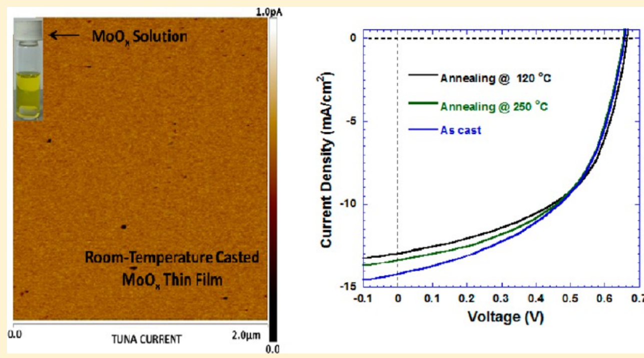

KEYWORDS: *polymer solar cells, hole extracting buffer layer, room-temperature processing, efficiency, stability, PEDOT/PSS replacement*

In the past two decades, bulk heterojunction (BHJ) polymer solar cells (PSCs) have been attracting intense attention due to their advantages over traditional inorganic solar cells such as flexibility, low-cost, lightweight, large area, clean and quiet, and processing simplicity.[1,2] In PSCs, BHJ composite is sandwiched between a poly(3,4-ethylenedioxythiophene) poly(styrenesulfonate) (PEDOT/PSS) coated indium tin oxide (ITO) anode and a low-work-function cathode, for example, calcium (Ca) or aluminum (Al); however, the acidic PEDOT/PSS etches ITO and causes PSCs degradation.[3,4] One possible solution to overcome these problems is to substitute PEDOT/PSS layer by using a stable metal oxide layer with suitable energy lever alignment between the ITO anode and BHJ active layer.[5,6]

Many metal oxides have been utilized as a hole extraction layer (HEL) in PSCs;[7−9] but the improvements in efficiency are still not sufficient. Molybdenum oxide is among all such metal oxide candidates and has been extensively studied for its transparency in visible range, good stability, and hole mobility.[10,11] The efficiencies of PSCs incorporating with vacuum-deposited metal oxides as a HEL were compatible to those using PEDOT/PSS as an anode buffer layer,[12] whereas the efficiencies of PSCs incorporating with solution-processed metal oxides were lower than those using PEDOT/PSS.[5,13,14] This is because the major challenges in widely used precursor methods for formation of metal oxide thin film with good hole transport properties usually require a thermal annealing at elevated temperature. Unfortunately, many plastic substrates that are used for fabricating polymer solar cells cannot sustain elevated annealing temperature due to subsequently reduced optical transparency and thermal and dimensional stability at high temperature.[15,16] In addition, high-temperature annealing large-area metal oxides is converse to the low-cost manufacturing PSCs. In answering the need for fabricating low-temperature, solution-processed PSCs with improved performance at low cost, a new method for processing metal oxides with thermal treatment at low temperature shall be realized and utilized.

In our previous work, we reported compatible efficiencies from PSCs with MoO_x thin film as a HEL compared to those using PEDOT/PSS as an anode buffer layer, where the sol−gel-derived MoO_x thin film has to be thermally annealed at 250 °C to ensure it has proper hole transporting properties.[10] In this paper, a water-free, room-temperature solution-processed MoO_x thin film as a HEL in PSCs was demonstrated. Such low-temperature processing will broaden the selection of substrates in future large scale PSC module production on plastic substrates, where processing temperature is a critical consideration.

The MoO_x thin film was spin-casted from MoO_x methanol solution which was prepared as follows: with vigorous stirring and effective radiating, 100 mL of H_2O_2 (concentration of 30%) was slowly added into 10 g molybdenum powder (CAS #7439−98−7, Alfa Aesar, Stock #00932, Lot #L13X018) in a clean beaker that sits in an ice−water bath to aid the radiating process. The obtained solution is then centrifuged to remove the rudimental substance. Clear solution is subsequently subjected to distillation to remove the solvent, H_2O and give dry MoO_x powder. Dried MoO_x power is dissolved in methanol for the preparation of MoO_x thin film.

Received: August 29, 2013
Published: February 4, 2014

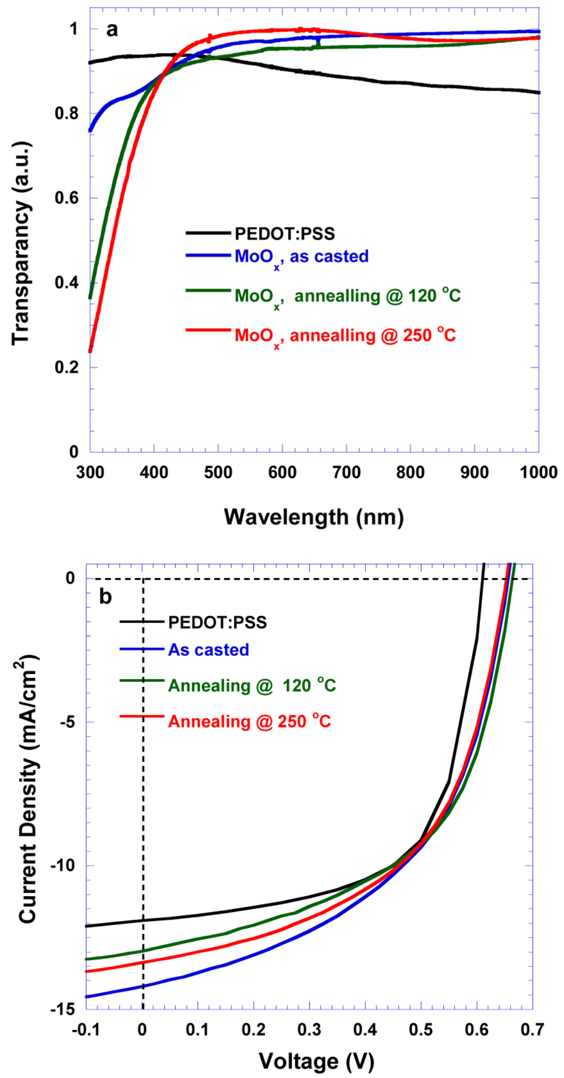

Figure 1. (a) Transparency spectra of MoO_x thin film annealed at different temperatures and PEDOT/PSS thin film; (b) Current-density versus voltage characterization of polymer solar cells using different anode buffer layers.

The transmission spectra of MoO_x thin films treated at different temperatures are shown in Figure 1a. The transmission spectrum of PEDOT/PSS thin layer is also presented in Figure 1a for comparison. A high transmittance in the visible range is desired when MoO_x thin film is expected to be a HEL inserted between the ITO anode and the BHJ composite layer. Greater than 90% transparency ranging from 500 to 1000 nm is observed from MoO_x thin films treated at different temperatures. The weak absorption from 800 to 900 nm is attributed to the free electrons being trapped by oxygen vacancies in MoO_x thin films.[17] Nevertheless, the transmittance of MoO_x thin films is higher than that of the PEDOT/PSS layer, indicating that MoO_x thin film is qualified to be a HEL through which more visible light is able to transmit from the ITO/MoO_x into the BHJ active layer without significant absorption losses.

The effect of MoO_x thin films on the device performance of PSCs was investigated using a device configuration of ITO/MoO_x/PTB7-F20:$PC_{71}BM$/Ca/Al and compared with the device performance from PSCs using PEDOT/PSS as an anode buffer layer. PTB7-F20 was novel narrow bandgap

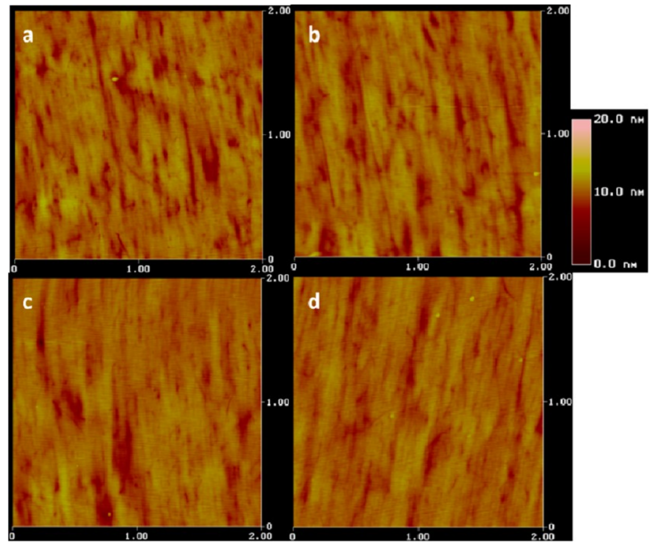

Figure 2. AFM images of bare ITO and MoO_x thin films: (a) bare ITO (RMS = 1.454 nm), (b) MoO_x as casted (RMS = 1.272 nm), (c) MoO_x thermal annealing at 120 °C (RMS = 1.637 nm), and MoO_x thermal annealing at 250 °C (RMS = 1.009 nm).

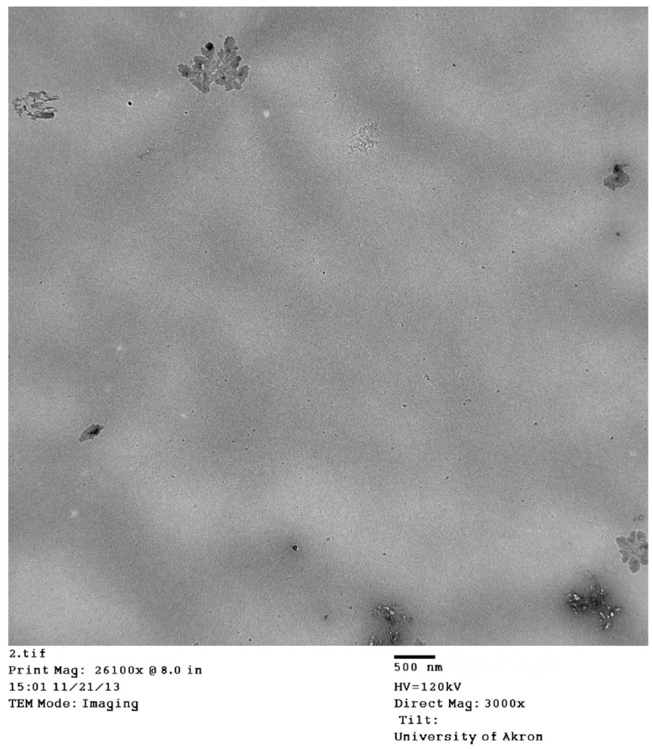

Figure 3. Imaging TEM result of MoO_x thin film spin-casted from 10 mg/mL methanol solution.

conjugated polymer and was reported elsewhere.[18] The $J-V$ curves of PSCs are shown in Figure 1b. Under AM1.5G illumination with the light intensity of 100 mW cm^{-2}, an open-circuit voltage (V_{OC}) of 0.60 V, a short-circuit current density (J_{SC}) of 11.92 $mAcm^{-2}$, a fill factor (FF) of 62%, and a corresponding PCE of 4.43% were obtained from PSCs by using PEDOT/PSS as an anode buffer layer. At the same condition, a V_{OC} of 0.65 V, a J_{SC} of 14.2 mA cm^{-2}, a FF of 50.7%, and a corresponding PCE of 4.67% were observed from PSCs by using MoO_x thin film without any treatment as a HEL.

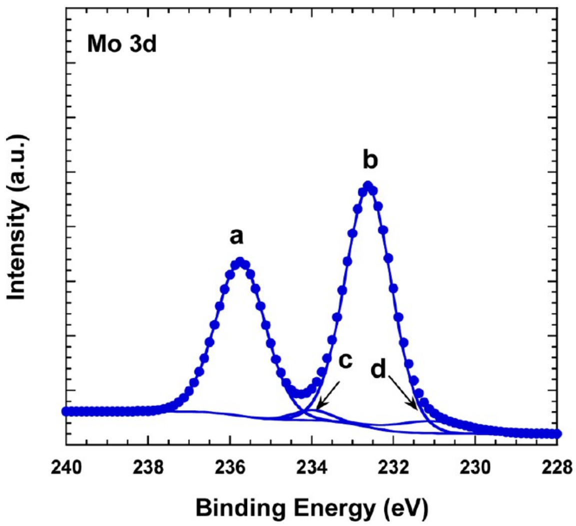

Figure 4. XPS spectra of Mo 3d core level from MoO_x thin film processed in room-temperature: major peaks, (a) Mo^{6+} (235.8 eV), (b) Mo^{6+} (235.8 eV); minor peaks, (c) Mo^{5+} (234.0 eV), (d) Mo^{5+} (231.1 eV).

For PSCs by using MoO_x thin film, which is annealed at 120 °C as a HEL, a V_{OC} of 0.67 V, a J_{SC} of 13.0 mA cm^{-2}, a FF of 52.8%, and a corresponding PCE of 4.62% were observed. For PSCs by using MoO_x thin film, which is annealed at 250 °C as a HEL, a V_{OC} of 0.65 V, a J_{SC} of 12.4 mA cm^{-2}, a FF of 53.2%, and a corresponding PCE of 4.63% were observed. Among these PSCs, PSCs with as casted MoO_x thin film as a HEL gave the best device performance.

In order to understand underlying device performance, we investigated surface morphology of MoO_x thin films by atomic force microscopy (AFM). Tapping mode AFM images of MoO_x thin films with different annealing conditions are shown in Figure 2. MoO_x thin films were spin-casted on precleaned ITO substrates. The root-mean-square (RMS) roughness of MoO_x thin film without any treatment is 1.272 nm, which is smaller than those from bare ITO (1.454 nm) and MoO_x thin film annealed at 120 °C (1.637 nm); however, it is larger than that from MoO_x thin film annealed at 120 °C (1.099 nm). The smooth surface implies that the BHJ composite layer can be easily deposited onto the top of MoO_x thin layer; consequently, PSCs with high efficiency is expected.

MoO_x thin film quality is investigated by using transmission electron microscopy (TEM). MoO_x thin films were spin-casted on carbon-coated copper grids from a high MoO_x concentration solution of 10 mg/mL in methanol. The obtained samples were dried in vacuum for 30 min before conducting the TEM study. The obtained TEM image is shown in Figure 3. It was found out that the MoO_x thin film shows a good uniformity. This result is attributed to the good solubility of the synthesized MoO_x powered in methanol, which will lead to the formation of a homogeneous solution for subsequent spin coating of a fine MoO_x thin film.

We further studied the stoichiometric composition of MoO_x thin films by X-ray photoelectron spectroscopy (XPS). Figure 4 presents XPS spectra of MoO_x thin film without any treatment. Decomposition of the XPS spectrum reveals two 3d doublets, which are corresponding to two different oxidation states, in the form of a Gaussian function for the Mo 3d spectrum. It is shown that the major peak appears at the binding energy of 232.6 and 235.8 eV are corresponded to 3d doublet of Mo^{6+}.[14] The minor peak is centered at 234 and 231.1 eV, which are typical values of 3d doublet of Mo^{5+}.[19] The molybdenum to oxygen stoichiometry data obtained from the XPS spectra of MoO_x thin films are summarized in Table 1. It revealed that the ratio of molybdenum to oxygen increases along with increased annealing temperatures, resulting in oxygen deficiency in MoO_x thin films at high annealing temperature.[20] Thus, the samples exhibit a more ideal MoO_3 lattice stoichiometry when annealed at lower temperatures, leading to a minimized Mo^{5+} and oxygen deficiency. The atomic concentration ratio of Mo^{5+} to Mo^{6+} obtained from room-temperature, processed MoO_x films is around 1:3.38, which indicates a less oxygen vacancies in MoO_x, resulting in high electrical conductivity. Because device performance is reversely related to the density of Mo^{5+} species in MoO_x thin films (with decreased Mo^{5+} and oxygen deficiency, the resulting device will have better performance),[20] room-temperature, processed MoO_x thin film will contribute to an increase in device performance.

We further measured the surface electrical conductivities of MoO_x thin films by peak force tapping tunneling AFM (PF-TUNA) module.[10,21] The probe was the PF-TUNA probe with spring constant of ∼0.5 N m^{-1} with 20 nm Pt/Ir coating on both front and rear. The spring currents were measured with bias voltage applied to the sample. The ramp rate of 0.4 Hz and the force set point of ∼60 nN were used for both thin films. The peak currents of MoO_x thin films without thermal annealing and with thermal annealing at 250 °C are shown in Figure 5. The surface electrical conductivity of MoO_x thin films with thermal annealed at 250 °C and without thermal annealing are 0.601 and 0.642 pA, respectively. Thus, surface electrical conductivity of MoOx thin film without any thermal annealing is higher than that of MoO_x thin films with thermal annealed at 250 °C. As a result, the efficiency from PSCs using MoO_x thin film without any thermal annealing as a HEL is higher than that using MoO_x thin films with thermal annealed at 250 °C .

In conclusion, room-temperature, solution-processed MoO_x thin film as a hole extraction layer to substitute PEDOT/PSS in polymer solar cells was demonstrated. The thin film of MoO_x shows a smoother surface, better transparency and high electrical conductivity than that of PEDOT/PSS thin layer and thus leading enhanced efficiency of PSCs than those using PEDOT/PSS anode buffer layer. These results demonstrated that the utilization of room-temperature, solution-processed

Table 1. XPS Compositional Analysis of Solution-Processed MoO_x Thin Films

	MoO_x, as spin-casted	MoO_x, annealing @ 120 °C	MoO_x, annealing @ 250 °C
molybdenum	15.1	20.8	22.0
oxygen	51.1	55.7	52.4
carbon	33.8	23.5	25.6
Mo/O ratio	1:3.38	1:2.67	1:2.38

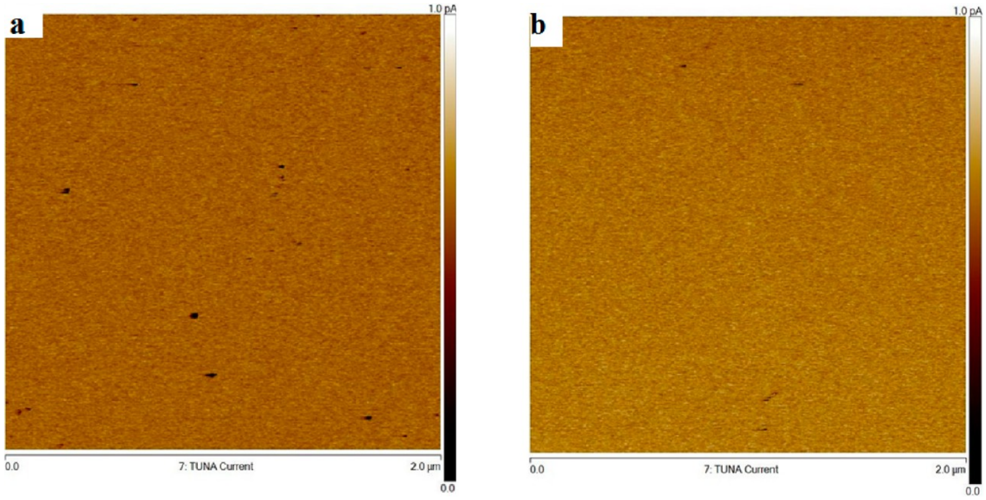

Figure 5. Peak current of MoO_x thin films: (a) without any treatment; (b) annealing at 250 °C.

MoO_x thin film as a hole extraction layer in polymer solar cells blaze a trail to achieve high performance devices.

■ AUTHOR INFORMATION

Corresponding Author

*E-mail: xgong@uakron.edu. Fax: (330) 972-4983.

Author Contributions

†These authors contributed equally to this work (B.L. and H.R.).

Notes

The authors declare no competing financial interest.

■ ACKNOWLEDGMENTS

The authors would like to thank NSF (1351785) for financial support.

■ REFERENCES

(1) Gunes, S.; Neugebauer, H.; Sariciftci, N. S. Conjugated polymer-based organic solar cells. *Chem. Rev.* **2007**, *107*, 1324−1338.

(2) Dennler, G.; Scharber, M. C.; Brabec, C. J. Polymer-fullerene bulk-heterojunction solar cells. *Adv. Mater.* **2009**, *21*, 1323−1338.

(3) de Jong, M. P.; van IJzendoorn, L. J.; de Voigt, M. J. A. Stability of the interface between indium-tin-oxide and poly(3,4-ethylenedioxythiophene)/poly(styrenesulfonate) in polymer light-emitting diodes. *Appl. Phys. Lett.* **2000**, *77*, 2255.

(4) Jorgensen, M.; Norrman, K.; Krebs, F. C. Stability/degradation of polymer solar cells. *Sol. Energy Mater. Sol. Cells* **2008**, *92*, 686−714.

(5) Kim, J. Y.; Kim, S. H.; Lee, H. H.; Lee, K.; Ma, W.; Gong, X.; Heeger, A. J. New architecture for high-efficiency polymer photovoltaic cells using solution-based titanium oxide as an optical spacer. *Adv. Mater.* **2006**, *18*, 572−576.

(6) Li, X.; Choy, W. C. H.; Xie, F.; Zhang, S.; Hou, J. Room-temperature solution-processed molybdenum oxide as a hole transport layer with Ag nanoparticles for highly efficient inverted organic solar cells. *J. Mater. Chem. A* **2013**, *1*, 6614−6621.

(7) Irwin, M. D.; Buchholz, D. B.; Hains, A. W.; Chang, R. P. H. *p*-Type semiconducting nickel oxide as an efficiency-enhancing anode interfacial layer in polymer bulk-heterojunction solar cells. *Proc. Natl. Acad. Sci. U.S.A.* **2008**, *105*, 2783−2787.

(8) Shrotriya, V.; Li, G.; Yao, Y.; Chu, C. W. Transition metal oxides as the buffer layer for polymer photovoltaic cells. *Appl. Phys. Lett.* **2006**, *88*, 073508.

(9) Chan, M. Y.; Lee, C. S.; Lai, S. L.; Fung, M. K.; Wong, F. L.; Sun, H. Y.; Lau, K. M.; Lee, S. T. Efficient organic photovoltaic devices using a combination of exciton blocking layer and anodic buffer layer. *J. Appl. Phys.* **2006**, *100*, 094506.

(10) Yang, T. B.; Wang, M.; Cao, Y.; Huang, F.; Huang, L.; Peng, J.; Gong, X.; Cheng, S. Z. D.; Cao, Y. Polymer solar cells with a low-temperature-annealed sol−gel-derived MoO_x film as a hole extraction layer. *Adv. Energy Mater.* **2012**, *2*, 523−527.

(11) Lee, Y.-J.; Yi, J.; Gao, G. F.; Koerner, H.; Park, K.; Wang, J.; Luo, K.; Vaia, R. A.; Hsu, J. W. P. Low-temperature solution-processed molybdenum oxide nanoparticle hole transport layers for organic photovoltaic devices. *Adv. Energy Mater.* **2012**, *2*, 1193−1197.

(12) Kyaw, A. K. K.; Sun, X. W.; Jiang, C. Y.; Lo, G. Q.; Zhao, D. W.; Kwong, D. L. An inverted organic solar cell employing a sol-gel derived ZnO electron selective layer and thermal evaporated MoO_3 hole selective layer. *Appl. Phys. Lett.* **2008**, *93*, 221107.

(13) Sun, Y.; Takacs, C. J.; Cowan, S. R.; Seo, J. H.; Gong, X.; Roy, A.; Heeger, A. J. Efficient, air-stable bulk heterojunction polymer solar cells using MoO_x as the anode interfacial layer. *Adv. Mater.* **2011**, *23*, 2226−2230.

(14) Stubhan, T.; Ameri, T.; Salinas, M.; Kranz, J.; Machui, F.; Halik, M.; Brabec, C. J. High shunt resistance in polymer solar cells comprising a MoO_3 hole extraction layer processed from nanoparticle suspension. *Appl. Phys. Lett.* **2011**, *98*, 253308.

(15) Chen, L. M.; Hong, Z.; Li, G.; Yang, Y. Recent progress in solar cells: manipulation of polymer:fullerene morphology and the formation of efficient inverted polymer solar cells. *Adv. Mater.* **2009**, *21*, 1434−1449.

(16) Crawford, G. P. *Flexible Flat Panel Display Technology*; John Wiley & Sons, Ltd: Chichester, U.K., 2005; p12.

(17) Deb, S. K.; Chopoorian, J. A. Optical properties and color-center formation in thin films of molybdenum trioxide. *J. Appl. Phys.* **1966**, *37*, 4818−4825.

(18) Wang, H.-X.; Yu, X. F.; Yi, C.; Ren, H.; Liu, C.; Yang, Y. L.; Xiao, S.; Zheng, J.; Karim, A.; Cheng, S. Z. D.; Gong, X. Fine-tuning of fluorinated thieno[3,4-*b*]thiophene copolymer for efficient polymer solar cells. *J. Phys. Chem. C* **2013**, *117*, 4358−4363.

(19) Zhu, J. H.; Cheng, Y. L.; Tang, K. J.; Wang, L. M.; Li, S. Q.; Yang, W. M. Synthesis of Ni−Mo and Co−Mo−Ni nano-sulfides and their stable catalysis on complicated full-ranged pyrolysis gasoline hydrorefinery. *RCS Adv.* **2012**, *2*, 8957−8961.

(20) Jasieniak, J. J.; Seifter, J.; Jo, J.; Mater, T.; Heeger, A. J. A Solution-processed MoO_x anode interlayer for use within organic photovoltaic devices. *Adv. Funct. Mater.* **2012**, *22*, 2594−2605.

(21) Yang, T. B.; Wang, M.; Duan, C. H.; Hu, X. W.; Huang, L.; Peng, J. B.; Huang, F.; Gong, X. Inverted polymer solar cells with 8.4% efficiency by conjugated polyelectrolyte. *Energy Environ. Sci.* **2012**, *5*, 8208−8214.